



HAL
open science

(E,E)-3-Methyl-2,5-bis(4-methylbenzylidene)cyclopentanone synthesis, characterization, Hirshfeld surface analysis and antibacterial activity

Fatiha Mahdi, Assia Sid, Rafika Bouchene, Paul Mosset, Thierry Roisnel

► **To cite this version:**

Fatiha Mahdi, Assia Sid, Rafika Bouchene, Paul Mosset, Thierry Roisnel. (E,E)-3-Methyl-2,5-bis(4-methylbenzylidene)cyclopentanone synthesis, characterization, Hirshfeld surface analysis and antibacterial activity. *Acta crystallographica Section E: Crystallographic communications* [2015-..], 2019, 75 (4), pp.506-+. 10.1107/S2056989019003827 . hal-02149780

HAL Id: hal-02149780

<https://univ-rennes.hal.science/hal-02149780>

Submitted on 9 Jul 2020

HAL is a multi-disciplinary open access archive for the deposit and dissemination of scientific research documents, whether they are published or not. The documents may come from teaching and research institutions in France or abroad, or from public or private research centers.

L'archive ouverte pluridisciplinaire **HAL**, est destinée au dépôt et à la diffusion de documents scientifiques de niveau recherche, publiés ou non, émanant des établissements d'enseignement et de recherche français ou étrangers, des laboratoires publics ou privés.



(E,E)-3-Methyl-2,5-bis(4-methylbenzylidene)cyclopentanone: synthesis, characterization, Hirshfeld surface analysis and antibacterial activity

Fatiha Mahdi,^a Assia Sid,^a Rafika Bouchene,^{b*} Paul Mosset^c and Thierry Roisnel^c

Received 10 December 2018

Accepted 19 March 2019

Edited by L. Fabian, University of East Anglia, England

Keywords: Claisen–Schmidt reaction; crossed-aldol condensation; crystal structure; spectroscopic studies.

CCDC reference: 1515960

Supporting information: this article has supporting information at journals.iucr.org/e

^aLaboratoire des Sciences Analytiques, Matériaux et Environnement (LSAME), Université Larbi Ben M'hidi, Oum El Bouaghi, 04000, Algeria, ^bDépartement Sciences de la Matière, Faculté des Sciences Exactes et Sciences de la Nature et de la Vie, Université Larbi Ben M'hidi, Oum El Bouaghi, 04000, Algeria, and ^cUniversité de Rennes 1, Institut des Sciences Chimiques de Rennes, CNRS UMR, 6226, Avenue du Général Leclerc, 35042 Rennes Cedex, France.

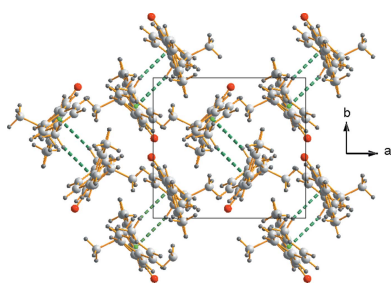
*Correspondence e-mail: wbouchene@yahoo.fr

The title compound, (*E,E*)-3-methyl-2,5-bis(4-methylbenzylidene)cyclopentanone (MBMCP), C₂₂H₂₂O, was obtained by Claisen–Schmidt condensation of 4-methylbenzaldehyde with 3-methylcyclopentanone in good yield. The structure of MBMCP was studied using UV, FT–IR and Raman spectroscopy, single-crystal X-ray diffraction (XRD) measurements, and ¹H and ¹³C nuclear magnetic resonance (NMR) spectroscopy. The molecular structure of MBMCP is fully extended in the *E,E* configuration. C–H···π stacking interactions play a significant role in the stabilization of the molecular packing. Hirshfeld surface analysis was used to quantify the non-covalent interactions in the crystal lattice. Microbiological studies were performed to investigate the antimicrobial activity of this new product.

1. Chemical context

The Claisen–Schmidt reaction has great importance in the synthesis of organic compounds (Rajput & Kaur, 2012), in particular in the synthesis of bis(substituted-benzylidene)cycloalkanones. This reaction is catalysed using strong acids (Dhar & Barton, 1981; Gall *et al.*, 1999) and base with or without solvents (Geissman & Clinton, 1946; Shan *et al.*, 2010). Recently, animal bone meal was used as a catalyst for crossed-aldol condensation (Riadi *et al.*, 2010). The preparation of β-chloro, β-bromo and α,β-unsaturated ketones from β-diketones has been carried out using Vilsmeier reagents (Mewshaw *et al.*, 1989). Numerous α,α'-bis(substituted-benzylidene)cycloalkanones exhibit biological activities (Robinson *et al.*, 2005; Piantadosi *et al.*, 1973). Furthermore, they are used as precursors for the preparation of biologically active heterocyclic compounds, such as pyrimidines (Deli *et al.*, 1984; Guilford *et al.*, 1999) and pyrazolines (Ziani *et al.*, 2013). These compounds have received a lot of attention because of their uses as perfume intermediates, pharmaceutical, agrochemical and liquid-crystal polymer units (Artico *et al.*, 1998; Amoozadeh *et al.*, 2010). α,α'-Bis(substituted-benzylidene)cycloalkanones are also essential pharmacophores of various natural products (Shetty *et al.*, 2015). An example of permitted therapeutic agents including this molecular framework is coumarin-chalcone (anticancer agents).

In the present work, we have synthesized, in one-step, (*E,E*)-3-methyl-2,5-bis(4-methylbenzylidene)cyclopentanone (MBMCP) by NaOH-catalysed Claisen–Schmidt condensation of 4-methyl benzaldehyde with 3-methyl cyclopentanone



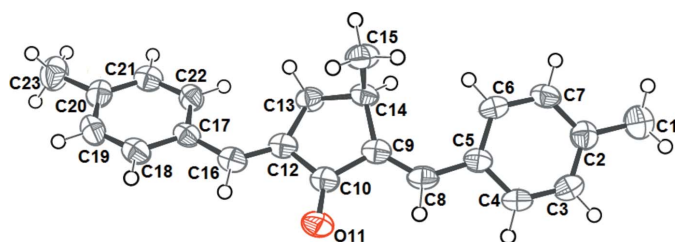
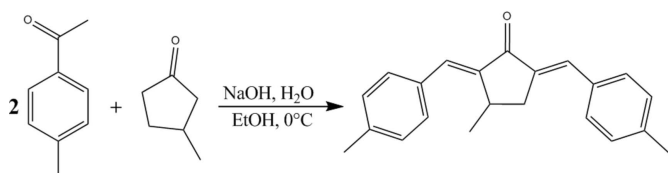


Figure 1
The asymmetric unit of MBMCP, showing the atom-numbering scheme. Displacement ellipsoids are drawn at the 50% probability level.

(see scheme). The structure of MBMCP was investigated by UV, FT-IR and Raman spectroscopy, single crystal X-ray diffraction (XRD) measurements and ^1H and ^{13}C nuclear magnetic resonance (NMR) spectroscopy.



Several studies on the biological activity of unsaturated carbonyl compounds have been carried out. As an example, a series of chalcone derivatives that mimic the essential properties of cationic antimicrobial peptides were designed and synthesized by Chu *et al.* (2018). The antibacterial activities of these chalcones against drug-sensitive bacteria, including *Staphylococcus aureus*, *Enterococcus faecalis*, *Escherichia coli* and *Salmonella enterica* indicate that these compounds have potential therapeutic effects against bacterial infections. The phenyl group and the fluoride atom in these compounds were found to play an important role in their antibacterial and hemolytic activities. The above findings prompted us to evaluate the antibacterial activity of MBMCP *in vitro* against four bacterial strains.

2. Structural commentary

The structure of MBMCP was confirmed using single X-ray diffraction. The asymmetric unit comprised a single molecule, illustrated in Fig. 1 with the atom-numbering scheme. The cyclopentanone ring adopts a half-chair form, with deviations of -0.146 (2) and 0.160 (2) Å from the mean plane of the ring for C13 and C14, respectively. The torsion angles within the five-membered ring are 4.7 (2) (C9-C10-C12-C13), -19.5 (2)° (C10-C12-C13-C14) and 26.3 (2)° (C12-C13-C14-C9), confirming the non-planarity of the central ring. The C15 methyl group in MBMCP lies practically perpendicular to the plane of its attached cyclopentanone ring, with torsion angle C12-C13-C14-C15 of -91.4 (2)°. The mean planes of the phenyl rings at either end of the molecule are twisted with respect to one another by 41.3 (1)°.

The C8=C9 and C12=C16 bond lengths are 1.344 (3) and 1.335 (3) Å, respectively, and those for C8-C5 and C16-C17 are 1.464 (3) and 1.462 (3) Å, respectively. These values are in between the normal values for single and double bonds (1.54 and 1.33 Å, respectively), which is consistent with a delocalized π -bonding system.

The molecular structure of MBMCP is fully extended in the *E,E* configuration stabilized by two short intramolecular contacts, $\text{H8}\cdots\text{O11}$ and $\text{H16}\cdots\text{O11}$ (2.55 and 2.53 Å, respectively).

3. Spectroscopic results

The FT-IR spectrum of MBMCP shows the strong band of a conjugated carbonyl group at 1670 cm^{-1} and two bands at 1616 and at 1596 cm^{-1} for the two non-equivalent exo-cyclic C=C bonds. The Raman spectrum shows two characteristic bands in the $1720\text{--}1670$ and $1620\text{--}1590\text{ cm}^{-1}$ regions, which indicate the presence of carbonyl groups conjugated with the double bonds.

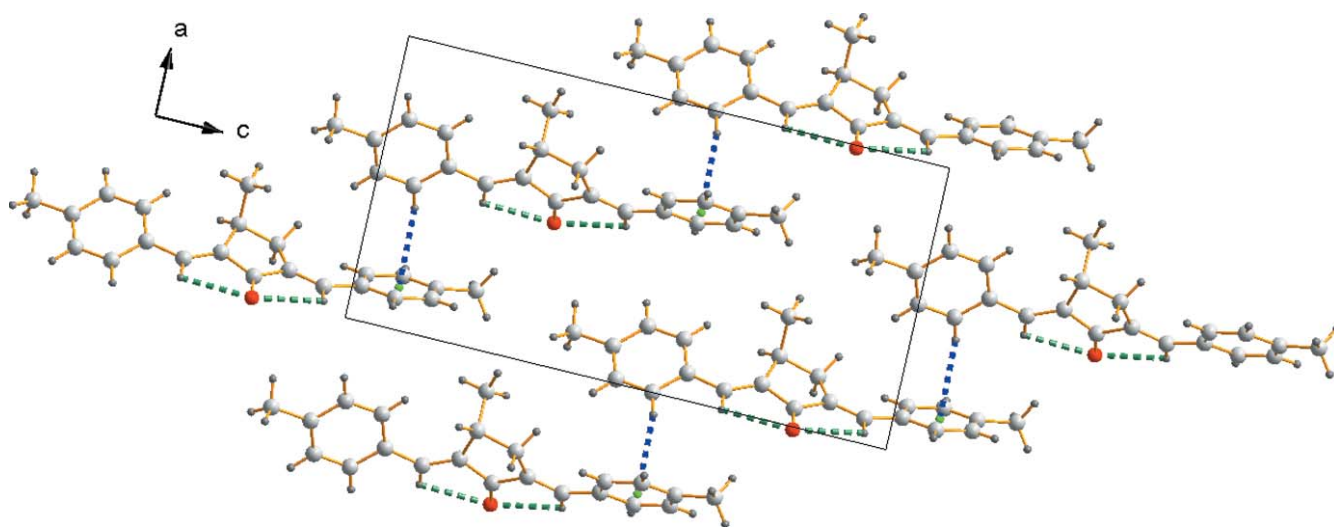


Figure 2
The one-dimensional chain structure of MBMCP formed *via* $\text{C-H}\cdots\pi$ interactions (blue dashed lines). The green spheres indicate the centroids of the phenyl ring.

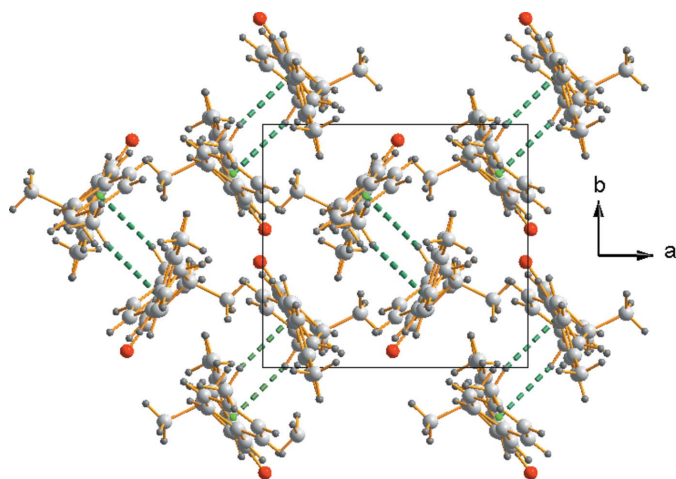


Figure 3
Crystal packing of MBMCP. The green spheres indicate the centroids of the phenyl ring.

The above result is also confirmed using the chemical shifts in the ^{13}C NMR spectrum for the carbonyl groups (196.46 ppm) and of the $\text{C}=\text{C}$ group at (139.7 and 139.8 ppm). The dienone of cyclic ketone derivatives occur in *E,E*, *Z,Z*, or *Z,E* configurations (Vatsadze *et al.*, 2006) and we have obtained the *E,E* isomer. The ^1H NMR spectrum shows the signals of CH protons at a greater field than 7.2 ppm ($\delta = 7.51\text{--}7.53$ ppm), which is in agreement with the *E* isomers, whereas the signals for the *Z* isomers are identified using the chemical shifts at $\delta \sim 6.8$ ppm (George & Roth, 1971).

The UV spectrum of the designated compound in ethanol reveals four absorption bands at 208 nm ($\epsilon = 3.215 \text{ L mol}^{-1}\text{cm}^{-1}$), 237 nm ($\epsilon = 1.984 \text{ L mol}^{-1}\text{cm}^{-1}$), 364 nm ($\epsilon = 3.215 \text{ L mol}^{-1}\text{cm}^{-1}$) and 376 nm ($\epsilon = 2.436 \text{ L mol}^{-1}\text{cm}^{-1}$) assigned to $n\text{--}\pi$, $\pi\text{--}\pi^*$ transitions.

4. Supramolecular features

Molecules of MBMCP pack with no classical hydrogen bonds. However, $\text{C18--H18}\cdots\text{O11}(1-x, -y, 1-z)$ and $\text{C23--H23B}\cdots\text{O11}(\frac{1}{2}+x, \frac{1}{2}-y, \frac{1}{2}+z)$ short contacts occur, where the oxygen atom of the carbonyl group works as an acceptor with $\text{O11}\cdots\text{H}$ distances of 2.61 and 2.66 Å, respectively. These

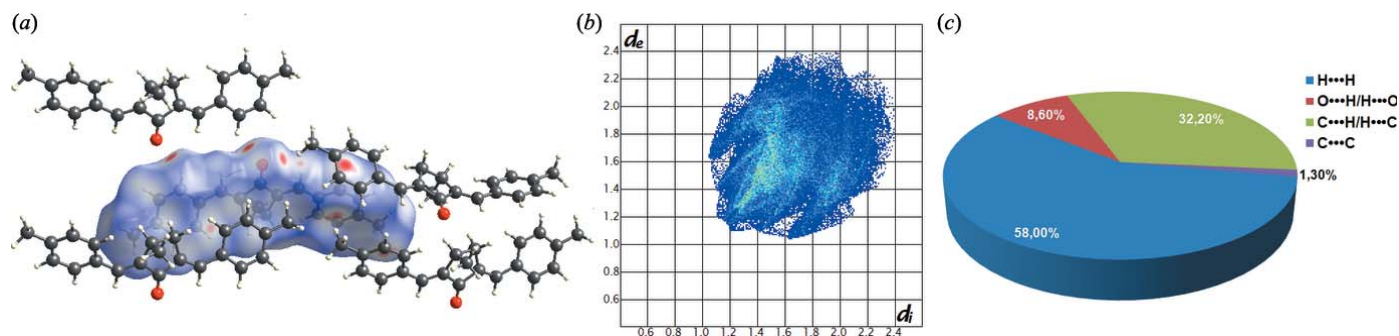


Figure 4
(a) View of the three-dimensional Hirshfeld surface mapped over d_{norm} , (b) the two-dimensional fingerprint plot and (c) the relative contributions to the Hirshfeld surface area by the various close intermolecular contacts in the structure of MBMCP.

Table 1
Hydrogen-bond geometry (Å, °).

*Cg*1 and *Cg*2 are the centroids of the C2–C7 and C17–C22 rings, respectively.

<i>D</i> –H \cdots <i>A</i>	<i>D</i> –H	H \cdots <i>A</i>	<i>D</i> \cdots <i>A</i>	<i>D</i> –H \cdots <i>A</i>
C1–H1C \cdots <i>Cg</i> 1 ⁱ	0.98	2.84	3.728 (3)	152
C4–H4 \cdots <i>Cg</i> 2 ⁱⁱ	0.95	2.75	3.574 (2)	146

Symmetry codes: (i) $-x + 1, -y + 1, -z$; (ii) $x - \frac{1}{2}, -y + \frac{1}{2}, z - \frac{1}{2}$.

interactions are neglected as the $\text{H}\cdots\text{O}$ van der Waals distance is 2.60 Å and $\text{C--H}\cdots\text{O}$ contacts frequently have $\text{H}\cdots\text{O}$ separations shorter than 2.4 Å (Taylor & Kennard, 1982). On the other hand, even though the carbonyl group is a strong acceptor, the O atom acts as a multiple acceptor. This condition corresponds to an important argument for the structural importance of the $\text{C--H}\cdots\text{O}$ hydrogen bond (Steiner, 1996).

Molecular chains of MBMCP propagate along the [101] direction through a $\text{C--H}\cdots\pi$ interaction (Table 1) involving the C4–H4 group of the C2–C7 phenyl ring pointing towards the π cloud on an adjacent C17–C22 ring, as shown in Fig. 2. The contact distances are consistent with those of the $\text{C--H}\cdots\pi$ edge-to-face interactions observed in the crystal structure of benzene (Bacon *et al.*, 1964).

The molecules of MBMCP stack in waves along the *a*-axis direction, as shown in Fig. 3. The methyl carbon (C1) makes an important contribution to the stability of this stacking arrangement *via* the establishment of a $\text{C--H}\cdots\pi$ interaction with the centroid of a neighboring aryl ring.

5. Hirshfeld surface analysis

The intermolecular interactions were quantified using Hirshfeld surface analysis (Fig. 4). The Hirshfeld surfaces of MBMCP, their associated two-dimensional fingerprint plots and relative contributions to the Hirshfeld surface area from the various close intermolecular contacts were calculated using *CrystalExplorer* software (Wolff *et al.*, 2007). The analysis of intermolecular interactions through the mapping of d_{norm} compares the contact distances d_i and d_e from the Hirshfeld surface to the nearest atom inside and outside, respectively, with their respective van der Waals radii. The red

Table 2
Antibacterial screening results (zone of inhibition, mm).

Compound	<i>Escherchia coli</i>	<i>Salmonella typhi</i>	<i>Staphylococcus aureus</i>	<i>Bacillus subtilis</i>
MBMCP	07	12	27	14
Penicillin	18	25	40	17
DMSO	–	–	–	–

(-) No antibacterial activity

regions represent contacts shorter than the sum of van der Waals radii, white regions represent intermolecular distances equal to van der Waals contacts and blue regions represent contacts longer than van der Waals radii.

As expected in organic compounds, the shortest and most abundant contacts for MBMCP are the H···H intermolecular interactions with a contribution to the Hirshfeld surface of 58%. The C···H contacts, which refer to the C–H··· π interactions described previously, contribute 32.2% of the Hirshfeld surfaces. On the shape-index surface, the C–H··· π interactions are clearly observed as red regions over the aromatic rings. The shape-index is in agreement with the 2D fingerprint plot, in which these interactions appear as two broad spikes both having $d_e + d_i \sim 2.7$ Å (Fig. 5). The large flat region, delineated by a blue outline on the curvedness of MBMCP reveals that π – π stacking interactions are absent.

6. Antibacterial activity

The antibacterial activity of MBMCP was assayed *in vitro* against *Escherchia coli*, *Staphylococcus aureus*, *Salmonella*

typhi and *Bacillus subtilis* via an agar cup-plate diffusion method (Barry, 1976; Ponce *et al.*, 2003). The bacteria tests were sub-cultured in Mueller–Hinton broth, from which 1 mL of cell suspension was taken and the optical density was adjusted to 0.5. The suspension was then spread as a thin film over the Mueller–Hinton agar plates. The synthetic compound was loaded onto discs with concentrations of 0.2, 0.3, 0.4 and 0.5 $\mu\text{g mL}^{-1}$ and air-dried. The dry discs were placed on the inoculated Mueller–Hinton agar plates and incubated at 310 K for 48 h. A penicillin disc (10 μg per disc) was used as the standard. A disc of 150 μl of DMSO served as the control. After incubation, the zone of inhibition (in mm) was measured and compared with that of penicillin for each concentration.

The antibacterial screening results are collected in Table 2. They reveal that the produced compound shows an antibacterial activity at MIC = 0.5 $\mu\text{g mL}^{-1}$ towards all the bacterial strains, but differs from one strain to another when comparing the zones of inhibition (mm). It exhibits moderate and promising activities against *Staphylococcus aureus* (27 mm) and *Bacillus subtilis* (14 mm). However, it shows low activities against *Escherchia coli* (7 mm) and *Salmonella typhi* (12 mm), which probably demonstrate that the produced compound exhibits a specific effect on those microorganisms.

7. Database survey

A search of the Cambridge Structural Database, CSD (Version 5.38; ConQuest 1.19; Groom *et al.*, 2016) revealed 20 derivatives of bis(benzylidene)cyclopentanone. The variety of compounds reported in the literature (Kawamata *et al.*, 1998; Nakhaei *et al.*, 2017) is due to substitution on the phenyl rings and/or on the cyclopentanone by different functional groups, such as hydroxy, methoxy, chlorine, fluorine *etc.*, and also by radicals. Cyclic conjugated *bis*(benzylidene)ketones have been reported to exhibit potent anti-inflammatory, antibacterial and antioxidant activity (Shetty *et al.*, 2015). *E,E*-2,5-dibenzylidene-3-methylcyclopentanone (DBMCP) is the nearest analogue to MBMCP. This molecule, like that of the title compound, exhibits a twisted five-membered ring, conveying modest non-planarity to the overall molecular shape with a maximum deviation from the mean plane of 0.44 Å (Theocharis *et al.*, 1984). The basic skeleton of this compound family, *E,E*-2,5-dibenzylidenecyclopentanone (DBCP), has been isolated in two polymorphic forms, exhibiting two different but nearly superimposable conformations (Arshad *et al.*, 2014). The previously reported polymorph I crystallizes in the orthorhombic $C222_1$ space group (Theocharis *et al.*, 1984), while the second form crystallizes in the monoclinic $P2_1$ space

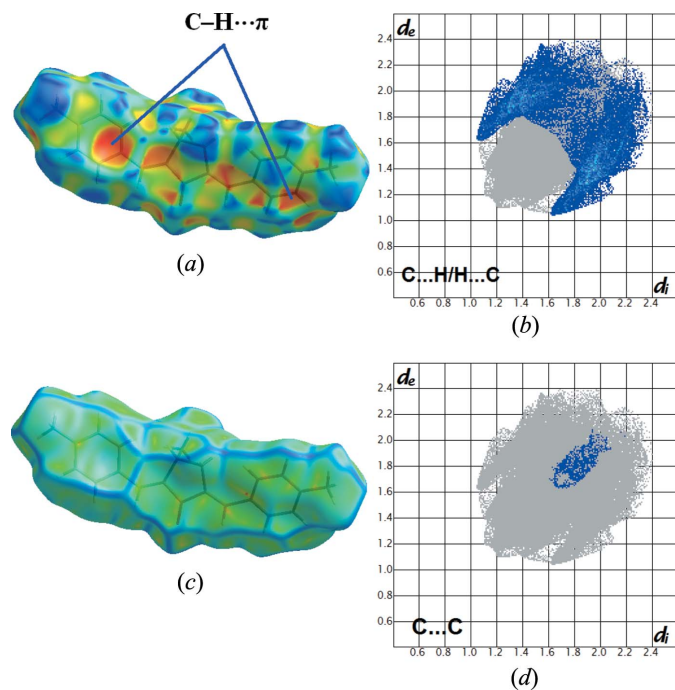


Figure 5
(a) The Hirshfeld surface mapped over shape-index, (b) the two-dimensional fingerprint plot for the H···C/C···H interactions, (c) the Hirshfeld surface mapped over curvedness and (d) the two-dimensional fingerprint plot for the C···C interactions in the title compound.

Table 3
Experimental details.

Crystal data	
Chemical formula	C ₂₂ H ₂₂ O
<i>M_r</i>	302.39
Crystal system, space group	Monoclinic, <i>P</i> 2 ₁ / <i>n</i>
Temperature (K)	150
<i>a</i> , <i>b</i> , <i>c</i> (Å)	9.8037 (9), 8.9815 (9), 18.8946 (17)
β (°)	90.985 (4)
<i>V</i> (Å ³)	1663.5 (3)
<i>Z</i>	4
Radiation type	Mo <i>K</i> α
μ (mm ⁻¹)	0.07
Crystal size (mm)	0.52 × 0.28 × 0.06
Data collection	
Diffractometer	Bruker D8 VENTURE
Absorption correction	Multi-scan (<i>SADABS</i> ; Bruker, 2014)
<i>T</i> _{min} , <i>T</i> _{max}	0.735, 0.996
No. of measured, independent and observed [<i>I</i> > 2 σ (<i>I</i>)] reflections	15325, 3808, 2471
<i>R</i> _{int}	0.115
Refinement	
<i>R</i> [<i>F</i> ² > 2 σ (<i>F</i> ²)], <i>wR</i> (<i>F</i> ²), <i>S</i>	0.070, 0.171, 1.12
No. of reflections	3808
No. of parameters	211
H-atom treatment	H-atom parameters constrained
$\Delta\rho_{\max}$, $\Delta\rho_{\min}$ (e Å ⁻³)	0.30, -0.26

Computer programs: *APEX3* (Bruker, 2015), *SAINT* (Bruker, 2014), *SHELXT* (Sheldrick, 2015a), *SHELXL2014* (Sheldrick, 2015b), *ORTEP-3 for Windows* (Farrugia, 2012), *DIAMOND* (Brandenburg & Berndt, 2001) and *CRYSCALC* (T. Roisnel, local program, version of 2015).

group. Both forms pack as supramolecular chains mainly stabilized by C–H···O, π – π and C–H··· π interactions and forming sheet-like multilayered structures.

8. Synthesis and crystallization

A mixture of 4-methylbenzaldehyde (20 mmol, 2 eq.) and 3-methylcyclopentanone (10 mmol, 1 eq.) were dissolved in ethanol (15 mL) into a flask (simple necked, round bottomed), and the solution was stirred for a few minutes at 273 K (ice bath). A solution of NaOH (10 mL, 40%) was added dropwise over several minutes into this mixture. The resulting mixture was stirred for 4 h approximately at room temperature. The obtained yellow precipitate was then filtered, washed with HCl (0.1 *N*) and cold water and then dried. The pure product was crystallized from ethanol solution at room temperature in 75% yield. Single crystals for X-ray diffraction were grown by slow solvent evaporation from a solution in ethanol.

The FT–IR spectrum of the compound was measured by the KBr pellet technique in the range of 4000–400 cm⁻¹, with a Nexus Nicolet FT–IR spectrometer at a resolution of 2 cm⁻¹. A Bruker Optik GmbH system was utilized to measure the Raman spectrum of the powder compound. A class 4 laser Raman spectrometer of 532 nm excitation from a diode laser (3B) was used with 2 cm⁻¹ resolution within the spectroscopic range 3500–0 cm⁻¹. ¹H and ¹³C NMR spectra were quantified with CDCl₃ using a (400.13 MHz in ¹H) Avance 400 Bruker spectrometer with TMS as internal standard.

¹H NMR (400 MHz, CDCl₃) δ (ppm): 1.23 (*d*, 1H, CH₃), 1.54 (*s*, 2H, H₂O), 2.39 (*s*, 6H, 2CH₃), 2.76 (*dd*, 1H_{cycle}), 3.18 (*ddd*, 1H_{cycle}), 3.66 (*m*, 1H_{cycle}), 7.22 (*d*, 2H_{aryl}), 7.25 (*d*, 2H_{aryl}), 7.47 (*d*, 3H_{aryl}), 7.51 (*s*, 1H_{ethylene}), 7.53 (*s*, 1H_{ethylene}), and 7.66 (*t*, 1H_{aryl}).

¹³C NMR (75.46 MHz, CDCl₃) δ (ppm): 21.03 (CH₃), 23.47 (CH₃), 23.49 (CH₃), 32.01 (CH_{cycle}), 35.98 (CH_{2cycle}), 129.51 (2C–Ar), 129.62 (2C–Ar), 130.71 (2C–Ar), 130.79 (2C–Ar), 133.37 (2C–Ar), 134.38 (2C–Ar), 135.57 (CH=C_{cycle}), 139.72 (C_{cycle}=CH), 139.76 (C_{cycle}=CH), 142.51 (CH=C_{cycle}), and 196.46 (C=O).

Fourier–transform infrared (FT–IR) spectroscopy (KBr, cm⁻¹): 3056–3022 (CH_{aromatic}), 2863 (CH_{aliphatic}), 1670 (C=O), 1616 and 1596 (C=C), and 1590.90, 1545.45 (C=C of aromatic rings).

Raman spectroscopy with 1000–1670 Hz frequency range for the C–C, C=C and C=O bonds. In addition, 2800–3156 Hz frequency domain for C–H bonds. Ultraviolet (UV) spectroscopy [EtOH, λ (nm)]: 208, 237 assignable to π – π , and 364, 376 assignable to π – π^* transitions.

9. Refinement

Crystal data, data collection and structure refinement details are summarized in Table 3. H atoms were included in their calculated positions and refined using the riding-atom approximation: C–H = 0.96 Å (methyl CH₃) and 0.93 Å (aryl), with *U*_{iso}(H) = 1.5*U*_{eq}(C) for methyl H atoms and 1.2*U*_{eq}(C) for all other H atoms.

Funding information

The authors acknowledge the Ministère de l'Enseignement Supérieur et de la Recherche Scientifique of Algeria for financial support.

References

- Amoozadeh, A., Rahmani, S. & Nemati, F. (2010). *S. Afr. J. Chem.* **63**, 72–74.
- Arshad, I., Ashraf, S., Abbas, A., Hameed, S., Lo, K. M. & Naseer, M. M. (2014). *Eur. Chem. Bull.* **3**, 587–592.
- Artico, M., Di Santo, R., Costi, R., Novellino, E., Greco, G., Massa, S., Tramontano, E., Marongiu, M. E., De Montis, A. & La Colla, P. (1998). *J. Med. Chem.* **41**, 3948–3960.
- Bacon, G. E., Curry, N. A. & Wilson, S. A. (1964). *Proc. R. Soc. London Ser. A*, **279**, 98–110.
- Barry, A. L. (1976). *Antimicrobial Susceptibility Test, Principle and Practice*, pp. 93–100. Philadelphia, USA: Illus Lea and Fehninger.
- Brandenburg, K. & Berndt, M. (2001). *DIAMOND*. Crystal Impact GbR, Bonn, Germany.
- Bruker (2014). *SAINT* and *SADABS*. Bruker AXS Inc., Madison, Wisconsin, USA.
- Bruker (2015). *APEX3*. Bruker AXS Inc., Madison, Wisconsin, USA.
- Chu, W. C., Bai, P. Y., Yang, Z. Q., Cui, D. Y., Hua, Y. G., Yang, Y., Yang, Q. Q., Zhang, E. & Qin, S. (2018). *Eur. J. Med. Chem.* **143**, 905–921.
- Deli, J., Lorand, T., Szabo, D. & Foldesi, A. (1984). *Pharmazie*, **39**, 539–540.
- Dhar, D. N. & Barton, D. (1981). *Chemistry of Chalcones and Related Compounds*, pp. 8–11. New York: Wiley.
- Farrugia, L. J. (2012). *J. Appl. Cryst.* **45**, 849–854.

- Gall, E. L., Texier-Boullet, F. & Hamelin, J. (1999). *Synth. Commun.* **29**, 3651–3657.
- Geissman, T. A. & Clinton, R. O. (1946). *J. Am. Chem. Soc.* **68**, 697–700.
- George, A. & Roth, H. J. (1971). *Tetrahedron Lett.* **12**, 4057–4060.
- Groom, C. R., Bruno, I. J., Lightfoot, M. P. & Ward, S. C. (2016). *Acta Cryst.* **B72**, 171–179.
- Guilford, W. J., Shaw, K. J., Dallas, J. L., Koovakkat, S., Lee, W., Liang, A., Light, D. R., McCarrick, M. A., Whitlow, M., Ye, B. & Morrissey, M. M. (1999). *J. Med. Chem.* **42**, 5415–5425.
- Rajput, J. K. & Kaur, G. (2012). *Tetrahedron Lett.* **53**, 646–649.
- Kawamata, J., Inoue, K. & Inabe, T. (1998). *Bull. Chem. Soc. Jpn.* **71**, 2777–2786.
- Mewshaw, R. E. (1989). *Tetrahedron Lett.* **30**, 3753–3756.
- Nakhaei, A., Morsali, A. & Davoodnia, A. (2017). *Russ. J. Gen. Chem.* **87**, 1073–1078.
- Piantadosi, C., Hall, I. H., Irvine, J. L. & Carlson, G. L. (1973). *J. Med. Chem.* **16**, 770–775.
- Ponce, A. G., Fritz, R., del Valle, C. E. & Roura, S. I. (2003). *LWT Food Sci. Technol.* **36**, 679–684.
- Riadi, Y., Mamouni, R., Azzalou, R., Boulahjar, R., Abrouki, Y., El Haddad, M., Routier, S., Guillaumet, G. & Lazar, S. (2010). *Tetrahedron Lett.* **51**, 6715–6717.
- Robinson, T. P., Hubbard, R. B. IV, Ehlers, T. J., Arbiser, J. L., Goldsmith, D. J. & Bowen, J. P. (2005). *Bioorg. Med. Chem.* **13**, 4007–4013.
- Shan, Z. X., Luo, X. X., Hu, L. & Hu, X. Y. (2010). *Sci. China: Chem.* **53**, 1095–1101.
- Sheldrick, G. M. (2015a). *Acta Cryst.* **A71**, 3–8.
- Sheldrick, G. M. (2015b). *Acta Cryst.* **C71**, 3–8.
- Shetty, D., Kim, Y. J., Shim, H. & Snyder, J. P. (2015). *Molecules*, **20**, 249–292.
- Steiner, T. (1996). *Crystallogr. Rev.* **6**, 1–51.
- Taylor, R. & Kennard, O. (1982). *J. Am. Chem. Soc.* **104**, 5063–5070.
- Theocharis, C. R., Jones, W., Thomas, J. M., Motevalli, M. & Hursthouse, M. B. (1984). *J. Chem. Soc. Perkin Trans. 2*, pp. 71–76.
- Vatsadze, S. Z., Manaenkova, M. A., Sviridenkova, N. V., Zyk, N. V., Krut'ko, D. P., Churakov, A. V., Antipin, Yu. M., Howard, J. A. K. & Lang, H. (2006). *Russ. Chem. Bull.* **55**, 1184–1194.
- Wolff, S. K., Grimwood, D. J., McKinnon, J. J., Jayatilaka, D. & Spackman, M. A. (2007). *Crystal Explorer*. University of Western Australia, Perth, Australia.
- Ziani, N., Lamara, K., Sid, A., Willem, Q., Dassonneville, B. & Demonceau, A. (2013). *Eur. J. Chem.* **4**, 176–179.

supporting information

Acta Cryst. (2019). E75, 506-511 [https://doi.org/10.1107/S2056989019003827]

(*E,E*)-3-Methyl-2,5-bis(4-methylbenzylidene)cyclopentanone: synthesis, characterization, Hirshfeld surface analysis and antibacterial activity

Fatiha Mahdi, Assia Sid, Rafika Bouchene, Paul Mosset and Thierry Roisnel

Computing details

Data collection: *SAINTE* (Bruker, 2014); cell refinement: *APEX3* (Bruker, 2015) and *SAINTE* (Bruker, 2014); data reduction: *SAINTE* (Bruker, 2014); program(s) used to solve structure: *SHELXT* (Sheldrick, 2015a); program(s) used to refine structure: *SHELXL2014* (Sheldrick, 2015b); molecular graphics: *ORTEP-3 for Windows* (Farrugia, 2012) and *DIAMOND* (Brandenburg & Berndt, 2001); software used to prepare material for publication: *CRYSCALC* (T. Roisnel, local program, version of 2015).

(*E,E*)-3-Methyl-2,5-bis(4-methylbenzylidene)cyclopentanone

Crystal data

$C_{22}H_{22}O$	$F(000) = 648$
$M_r = 302.39$	$D_x = 1.207 \text{ Mg m}^{-3}$
Monoclinic, $P2_1/n$	Mo $K\alpha$ radiation, $\lambda = 0.71073 \text{ \AA}$
$a = 9.8037 (9) \text{ \AA}$	Cell parameters from 2848 reflections
$b = 8.9815 (9) \text{ \AA}$	$\theta = 2.4\text{--}27.4^\circ$
$c = 18.8946 (17) \text{ \AA}$	$\mu = 0.07 \text{ mm}^{-1}$
$\beta = 90.985 (4)^\circ$	$T = 150 \text{ K}$
$V = 1663.5 (3) \text{ \AA}^3$	Thick plate, colourless
$Z = 4$	$0.52 \times 0.28 \times 0.06 \text{ mm}$

Data collection

Bruker D8 VENTURE diffractometer	15325 measured reflections
Radiation source: Incoatec microfocus sealed tube	3808 independent reflections
Multilayer monochromator	2471 reflections with $I > 2\sigma(I)$
rotation images scans	$R_{\text{int}} = 0.115$
Absorption correction: multi-scan (SADABS; Bruker, 2014)	$\theta_{\text{max}} = 27.5^\circ$, $\theta_{\text{min}} = 3.1^\circ$
$T_{\text{min}} = 0.735$, $T_{\text{max}} = 0.996$	$h = -12 \rightarrow 12$
	$k = -11 \rightarrow 10$
	$l = -24 \rightarrow 24$

Refinement

Refinement on F^2	0 restraints
Least-squares matrix: full	Primary atom site location: structure-invariant direct methods
$R[F^2 > 2\sigma(F^2)] = 0.070$	Secondary atom site location: difference Fourier map
$wR(F^2) = 0.171$	Hydrogen site location: inferred from neighbouring sites
$S = 1.12$	
3808 reflections	
211 parameters	

H-atom parameters constrained
 $w = 1/[\sigma^2(F_o^2) + (0.0652P)^2 + 0.431P]$
 where $P = (F_o^2 + 2F_c^2)/3$

$(\Delta/\sigma)_{\max} = 0.005$
 $\Delta\rho_{\max} = 0.30 \text{ e } \text{\AA}^{-3}$
 $\Delta\rho_{\min} = -0.26 \text{ e } \text{\AA}^{-3}$

Special details

Geometry. All esds (except the esd in the dihedral angle between two l.s. planes) are estimated using the full covariance matrix. The cell esds are taken into account individually in the estimation of esds in distances, angles and torsion angles; correlations between esds in cell parameters are only used when they are defined by crystal symmetry. An approximate (isotropic) treatment of cell esds is used for estimating esds involving l.s. planes.

Refinement. Refinement of F^2 against ALL reflections. The weighted R-factor wR and goodness of fit S are based on F^2 , conventional R-factors R are based on F, with F set to zero for negative F^2 . The threshold expression of $F^2 > 2\text{sigma}(F^2)$ is used only for calculating R-factors(gt) etc. and is not relevant to the choice of reflections for refinement. R-factors based on F^2 are statistically about twice as large as those based on F, and R-factors based on ALL data will be even larger.

Fractional atomic coordinates and isotropic or equivalent isotropic displacement parameters (\AA^2)

	x	y	z	$U_{\text{iso}}^*/U_{\text{eq}}$
C1	0.6385 (3)	0.4045 (3)	-0.09361 (12)	0.0385 (6)
H1A	0.6054	0.3291	-0.1273	0.058*
H1B	0.7347	0.4259	-0.1025	0.058*
H1C	0.5848	0.4958	-0.0994	0.058*
C2	0.6242 (2)	0.3472 (3)	-0.01957 (12)	0.0274 (5)
C3	0.5158 (2)	0.2568 (3)	-0.00074 (13)	0.0357 (6)
H3	0.4503	0.2287	-0.0359	0.043*
C4	0.5009 (2)	0.2070 (3)	0.06766 (12)	0.0316 (6)
H4	0.4260	0.1443	0.0785	0.038*
C5	0.5940 (2)	0.2468 (2)	0.12164 (11)	0.0227 (5)
C6	0.7056 (2)	0.3345 (3)	0.10266 (12)	0.0286 (5)
H6	0.7722	0.3611	0.1375	0.034*
C7	0.7195 (2)	0.3824 (3)	0.03386 (12)	0.0308 (6)
H7	0.7964	0.4414	0.0223	0.037*
C8	0.5659 (2)	0.1961 (3)	0.19360 (12)	0.0242 (5)
H8	0.4994	0.1195	0.1962	0.029*
C9	0.6180 (2)	0.2391 (2)	0.25660 (12)	0.0226 (5)
C10	0.5636 (2)	0.1772 (2)	0.32316 (12)	0.0232 (5)
O11	0.49025 (16)	0.06702 (19)	0.32852 (8)	0.0328 (4)
C12	0.6133 (2)	0.2716 (2)	0.38293 (12)	0.0228 (5)
C13	0.6898 (2)	0.4010 (2)	0.35203 (11)	0.0244 (5)
H13A	0.7731	0.4227	0.3805	0.029*
H13B	0.6318	0.4913	0.3506	0.029*
C14	0.7269 (2)	0.3520 (2)	0.27653 (12)	0.0235 (5)
H14	0.7247	0.4386	0.2433	0.028*
C15	0.8679 (2)	0.2773 (3)	0.27741 (13)	0.0315 (6)
H15A	0.8700	0.1980	0.3130	0.047*
H15B	0.9381	0.3515	0.2891	0.047*
H15C	0.8856	0.2349	0.2307	0.047*
C16	0.5869 (2)	0.2357 (2)	0.44987 (11)	0.0236 (5)
H16	0.5378	0.1453	0.4553	0.028*
C17	0.6207 (2)	0.3119 (2)	0.51624 (11)	0.0230 (5)

C18	0.6069 (2)	0.2345 (3)	0.57982 (12)	0.0262 (5)
H18	0.5783	0.1335	0.5787	0.031*
C19	0.6338 (2)	0.3014 (3)	0.64411 (12)	0.0288 (6)
H19	0.6255	0.2451	0.6864	0.035*
C20	0.6730 (2)	0.4508 (3)	0.64823 (12)	0.0269 (5)
C21	0.6866 (2)	0.5284 (3)	0.58517 (12)	0.0274 (5)
H21	0.7138	0.6299	0.5866	0.033*
C22	0.6614 (2)	0.4612 (3)	0.52014 (12)	0.0247 (5)
H22	0.6718	0.5170	0.4779	0.030*
C23	0.6981 (3)	0.5255 (3)	0.71853 (13)	0.0394 (7)
H23A	0.7168	0.6314	0.7110	0.059*
H23B	0.7766	0.4790	0.7425	0.059*
H23C	0.6172	0.5147	0.7478	0.059*

Atomic displacement parameters (Å²)

	U^{11}	U^{22}	U^{33}	U^{12}	U^{13}	U^{23}
C1	0.0416 (15)	0.0411 (16)	0.0330 (14)	−0.0006 (12)	0.0010 (11)	0.0032 (12)
C2	0.0267 (12)	0.0281 (13)	0.0273 (12)	0.0035 (10)	0.0014 (10)	−0.0004 (10)
C3	0.0260 (12)	0.0494 (17)	0.0314 (14)	−0.0082 (11)	−0.0056 (10)	−0.0007 (12)
C4	0.0218 (12)	0.0392 (15)	0.0338 (14)	−0.0112 (10)	0.0002 (10)	−0.0009 (11)
C5	0.0189 (10)	0.0199 (11)	0.0293 (12)	0.0013 (9)	0.0013 (9)	0.0003 (9)
C6	0.0218 (11)	0.0329 (14)	0.0309 (13)	−0.0075 (10)	−0.0032 (9)	−0.0017 (11)
C7	0.0279 (12)	0.0310 (14)	0.0337 (13)	−0.0112 (10)	0.0049 (10)	0.0000 (11)
C8	0.0168 (10)	0.0214 (12)	0.0346 (13)	0.0001 (9)	0.0000 (9)	0.0012 (10)
C9	0.0180 (10)	0.0180 (11)	0.0318 (12)	0.0041 (8)	0.0001 (9)	0.0022 (10)
C10	0.0198 (11)	0.0198 (11)	0.0299 (12)	0.0018 (9)	−0.0011 (9)	0.0049 (10)
O11	0.0343 (9)	0.0284 (9)	0.0357 (10)	−0.0127 (8)	−0.0001 (7)	0.0056 (8)
C12	0.0191 (10)	0.0178 (11)	0.0314 (12)	0.0040 (8)	−0.0008 (9)	0.0037 (10)
C13	0.0240 (11)	0.0192 (12)	0.0298 (12)	−0.0016 (9)	−0.0013 (9)	0.0019 (10)
C14	0.0202 (11)	0.0203 (12)	0.0299 (12)	−0.0027 (9)	0.0016 (9)	0.0031 (10)
C15	0.0212 (11)	0.0354 (15)	0.0380 (14)	−0.0036 (10)	−0.0009 (10)	−0.0031 (11)
C16	0.0205 (11)	0.0180 (11)	0.0323 (13)	0.0033 (9)	0.0017 (9)	0.0041 (10)
C17	0.0168 (10)	0.0234 (12)	0.0289 (12)	0.0040 (9)	0.0029 (9)	0.0053 (10)
C18	0.0208 (11)	0.0248 (13)	0.0331 (13)	0.0035 (9)	0.0032 (9)	0.0065 (10)
C19	0.0222 (11)	0.0374 (14)	0.0271 (13)	0.0108 (10)	0.0050 (9)	0.0104 (11)
C20	0.0164 (10)	0.0387 (14)	0.0258 (12)	0.0111 (10)	0.0011 (9)	−0.0002 (11)
C21	0.0223 (11)	0.0247 (13)	0.0352 (14)	0.0049 (9)	0.0017 (10)	0.0018 (10)
C22	0.0227 (11)	0.0263 (13)	0.0252 (12)	0.0043 (9)	0.0005 (9)	0.0061 (10)
C23	0.0380 (14)	0.0501 (17)	0.0302 (14)	0.0100 (12)	0.0005 (11)	−0.0021 (12)

Geometric parameters (Å, °)

C1—C2	1.499 (3)	C13—H13A	0.9900
C1—H1A	0.9800	C13—H13B	0.9900
C1—H1B	0.9800	C14—C15	1.536 (3)
C1—H1C	0.9800	C14—H14	1.0000
C2—C3	1.388 (3)	C15—H15A	0.9800

C2—C7	1.400 (3)	C15—H15B	0.9800
C3—C4	1.378 (3)	C15—H15C	0.9800
C3—H3	0.9500	C16—C17	1.462 (3)
C4—C5	1.404 (3)	C16—H16	0.9500
C4—H4	0.9500	C17—C18	1.396 (3)
C5—C6	1.399 (3)	C17—C22	1.401 (3)
C5—C8	1.464 (3)	C18—C19	1.377 (3)
C6—C7	1.379 (3)	C18—H18	0.9500
C6—H6	0.9500	C19—C20	1.398 (4)
C7—H7	0.9500	C19—H19	0.9500
C8—C9	1.344 (3)	C20—C21	1.389 (3)
C8—H8	0.9500	C20—C23	1.504 (3)
C9—C10	1.483 (3)	C21—C22	1.387 (3)
C9—C14	1.515 (3)	C21—H21	0.9500
C10—O11	1.228 (3)	C22—H22	0.9500
C10—C12	1.488 (3)	C23—H23A	0.9800
C12—C16	1.335 (3)	C23—H23B	0.9800
C12—C13	1.506 (3)	C23—H23C	0.9800
C13—C14	1.543 (3)		
C2—C1—H1A	109.5	H13A—C13—H13B	108.8
C2—C1—H1B	109.5	C9—C14—C15	109.94 (18)
H1A—C1—H1B	109.5	C9—C14—C13	104.13 (17)
C2—C1—H1C	109.5	C15—C14—C13	109.97 (18)
H1A—C1—H1C	109.5	C9—C14—H14	110.9
H1B—C1—H1C	109.5	C15—C14—H14	110.9
C3—C2—C7	116.8 (2)	C13—C14—H14	110.9
C3—C2—C1	121.6 (2)	C14—C15—H15A	109.5
C7—C2—C1	121.6 (2)	C14—C15—H15B	109.5
C4—C3—C2	121.6 (2)	H15A—C15—H15B	109.5
C4—C3—H3	119.2	C14—C15—H15C	109.5
C2—C3—H3	119.2	H15A—C15—H15C	109.5
C3—C4—C5	121.4 (2)	H15B—C15—H15C	109.5
C3—C4—H4	119.3	C12—C16—C17	130.9 (2)
C5—C4—H4	119.3	C12—C16—H16	114.6
C6—C5—C4	117.3 (2)	C17—C16—H16	114.6
C6—C5—C8	125.0 (2)	C18—C17—C22	117.6 (2)
C4—C5—C8	117.7 (2)	C18—C17—C16	118.7 (2)
C7—C6—C5	120.5 (2)	C22—C17—C16	123.6 (2)
C7—C6—H6	119.7	C19—C18—C17	121.5 (2)
C5—C6—H6	119.7	C19—C18—H18	119.3
C6—C7—C2	122.3 (2)	C17—C18—H18	119.3
C6—C7—H7	118.9	C18—C19—C20	121.1 (2)
C2—C7—H7	118.9	C18—C19—H19	119.5
C9—C8—C5	131.2 (2)	C20—C19—H19	119.5
C9—C8—H8	114.4	C21—C20—C19	117.7 (2)
C5—C8—H8	114.4	C21—C20—C23	121.1 (2)
C8—C9—C10	120.4 (2)	C19—C20—C23	121.2 (2)

C8—C9—C14	131.9 (2)	C22—C21—C20	121.6 (2)
C10—C9—C14	107.62 (18)	C22—C21—H21	119.2
O11—C10—C9	126.3 (2)	C20—C21—H21	119.2
O11—C10—C12	125.5 (2)	C21—C22—C17	120.6 (2)
C9—C10—C12	108.17 (19)	C21—C22—H22	119.7
C16—C12—C10	121.0 (2)	C17—C22—H22	119.7
C16—C12—C13	131.3 (2)	C20—C23—H23A	109.5
C10—C12—C13	107.73 (18)	C20—C23—H23B	109.5
C12—C13—C14	105.37 (18)	H23A—C23—H23B	109.5
C12—C13—H13A	110.7	C20—C23—H23C	109.5
C14—C13—H13A	110.7	H23A—C23—H23C	109.5
C12—C13—H13B	110.7	H23B—C23—H23C	109.5
C14—C13—H13B	110.7		
C7—C2—C3—C4	1.4 (4)	C16—C12—C13—C14	160.9 (2)
C1—C2—C3—C4	-178.5 (2)	C10—C12—C13—C14	-19.5 (2)
C2—C3—C4—C5	0.8 (4)	C8—C9—C14—C15	-88.7 (3)
C3—C4—C5—C6	-2.4 (4)	C10—C9—C14—C15	93.9 (2)
C3—C4—C5—C8	176.5 (2)	C8—C9—C14—C13	153.5 (2)
C4—C5—C6—C7	1.9 (3)	C10—C9—C14—C13	-23.9 (2)
C8—C5—C6—C7	-176.9 (2)	C12—C13—C14—C9	26.3 (2)
C5—C6—C7—C2	0.3 (4)	C12—C13—C14—C15	-91.4 (2)
C3—C2—C7—C6	-2.0 (4)	C10—C12—C16—C17	-178.0 (2)
C1—C2—C7—C6	178.0 (2)	C13—C12—C16—C17	1.6 (4)
C6—C5—C8—C9	13.9 (4)	C12—C16—C17—C18	-166.3 (2)
C4—C5—C8—C9	-164.9 (2)	C12—C16—C17—C22	16.4 (4)
C5—C8—C9—C10	175.1 (2)	C22—C17—C18—C19	-0.8 (3)
C5—C8—C9—C14	-2.0 (4)	C16—C17—C18—C19	-178.30 (19)
C8—C9—C10—O11	14.6 (3)	C17—C18—C19—C20	1.5 (3)
C14—C9—C10—O11	-167.6 (2)	C18—C19—C20—C21	-1.3 (3)
C8—C9—C10—C12	-165.43 (19)	C18—C19—C20—C23	178.0 (2)
C14—C9—C10—C12	12.3 (2)	C19—C20—C21—C22	0.4 (3)
O11—C10—C12—C16	4.3 (3)	C23—C20—C21—C22	-178.8 (2)
C9—C10—C12—C16	-175.62 (19)	C20—C21—C22—C17	0.2 (3)
O11—C10—C12—C13	-175.4 (2)	C18—C17—C22—C21	0.0 (3)
C9—C10—C12—C13	4.7 (2)	C16—C17—C22—C21	177.3 (2)

Hydrogen-bond geometry (\AA , $^\circ$)

$Cg1$ and $Cg2$ are the centroids of the C2—C7 and C17—C22 rings, respectively.

$D-H\cdots A$	$D-H$	$H\cdots A$	$D\cdots A$	$D-H\cdots A$
C1—H1C \cdots $Cg1^i$	0.98	2.84	3.728 (3)	152
C4—H4 \cdots $Cg2^{ii}$	0.95	2.75	3.574 (2)	146

Symmetry codes: (i) $-x+1, -y+1, -z$; (ii) $x-1/2, -y+1/2, z-1/2$.